RSC Advances

PAPER

View Article Online
View Journal | View Issue

Cite this: *RSC Adv.*, 2025, **15**, 32263

Solid-phase synthesis of polyunsaturated fatty acids facilitates precise structural investigation on FFAR1/4 agonist activities and the inhibition of neutrophil pseudopod formation

Yaohong Shi,[a] Yutaro Saito, *[a] Masashi Hotta,[b] Mayuko Akita,[a] Akiharu Uwamizu,[c] Junken Aoki,[c] Jun Kunisawa[bdefg] and Shinsuke Sando *[ah]

Received 7th July 2025
Accepted 18th August 2025

DOI: 10.1039/d5ra04836b

rsc.li/rsc-advances

Polyunsaturated fatty acids (PUFAs), fatty acids with multiple unsaturated carbon–carbon bonds, constitute a crucial class of lipids. While the vast diversity of PUFA species arises from their structural variations, most of them are poorly investigated due to their limited availability. Here, we utilize solid-phase synthesis of PUFAs, which we have recently developed, to construct a PUFA library. With the library, we investigate agonist activities for free fatty acid receptors 1 (FFAR1) and 4 (FFAR4), inhibition abilities against neutrophil pseudopod formation, and anti-inflammatory effects on the hypersensitivity mouse model. This study highlights the utility of PUFA solid-phase synthesis as a powerful approach for elucidating the relationship between the chemical structures of PUFAs and their biological functions.

Introduction

Polyunsaturated fatty acids (PUFAs) are fatty acids characterized by multiple unsaturated carbon–carbon bonds and constitute a crucial class of lipids.[1] The remarkable diversity of PUFA species arises from variations in carbon chain length, degree of unsaturation, and the positional distribution of double bonds. Subtle structural differences among these molecules result in distinct physicochemical properties and biological functions. While well-studied PUFAs such as eicosapentaenoic acid (EPA, **1**) and arachidonic acid (ARA, **2**) are naturally abundant and readily accessible,[2,3] many others remain scarce and poorly investigated. Notably, in recent years, the application of advanced lipidomic analyses has led to the successive identification of rare PUFAs with extremely low natural abundance. In this context, investigating chemically fine-tuned PUFAs is essential to elucidate how their structural variations influence biological function and contribute to the functional diversity.

The chemical structure of a typical PUFA can be divided into three moieties, as shown in Fig. 1A. Head moiety comprises a carboxyl group and a saturated fatty chain. Middle moiety consists of an unsaturated fatty chain with sequential methylene-interrupted *Z*-olefins. Tail moiety is a terminal alkyl chain. Here, we define these three structural components using the following parameters: head moiety: δ, representing the number of carbon atoms from the carboxyl carbon to the first olefin; middle moiety: π, indicating the number of olefins; and tail moiety: ω, denoting the number of carbon atoms from the terminal methyl group to the closest olefin. For instance, EPA (**1**) is expressed as $[\delta,\pi,\omega] = [5,5,3]$.

Free fatty acid receptors 1 (FFAR1, GPR40) and 4 (FFAR4, GPR120) are G protein-coupled receptors (GPCRs) with attractive attention as potential therapeutic targets for various diseases, including type-2 diabetes, autoimmune disorders, neurodegenerative diseases, and cancers.[4,5] FFAR1/4 agonists have been extensively studied and remain challenging targets for drug development and disease prevention.[6,7] These receptors are activated by a wide range of medium- and long-chain fatty acids.[3,8–10] PUFAs are recognized as their natural agonists, contributing to health maintenance through dietary intake and supplementation.

[a]*Department of Chemistry and Biotechnology, Graduate School of Engineering, The University of Tokyo, 7-3-1 Hongo, Bunkyo-ku, Tokyo 113-8656, Japan. E-mail: saito.y@chembio.t.u-tokyo.ac.jp; ssando@chembio.t.u-tokyo.ac.jp*

[b]*Laboratory of Vaccine Materials, Laboratory of Gut Environmental System, Microbial Research Center for Health and Medicine, National Institutes of Biomedical Innovation, Health and Nutrition (NIBN), 7-6-8 Asagi Saito, Osaka 567-0085, Ibaraki, Japan*

[c]*Department of Health Chemistry, Graduate School of Pharmaceutical Sciences, The University of Tokyo, Bunkyo-ku, Tokyo, Japan*

[d]*Department of Microbiology and Immunology, Kobe University Graduate School of Medicine, 7-5-1 Kusunoki-cho, Chuo-ku, Kobe, Hyogo 650-0017, Japan*

[e]*International Vaccine Design Center, The Institute of Medical Science, The University of Tokyo, 4-6-1 Shirokanedai, Minato-ku, Tokyo 108-8639, Japan*

[f]*Graduate School of Medicine, Graduate School of Dentistry, Graduate School of Pharmaceutical Sciences, Department of Science, The University of Osaka, 1-1 Yamadaoka, Suita, Osaka 565-0871, Japan*

[g]*Research Organization for Nano and Life Innovation, Waseda University, Tokyo, Japan*

[h]*Department of Bioengineering, Graduate School of Engineering, The University of Tokyo, 7-3-1 Hongo, Bunkyo-ku, Tokyo, 113-8656, Japan*

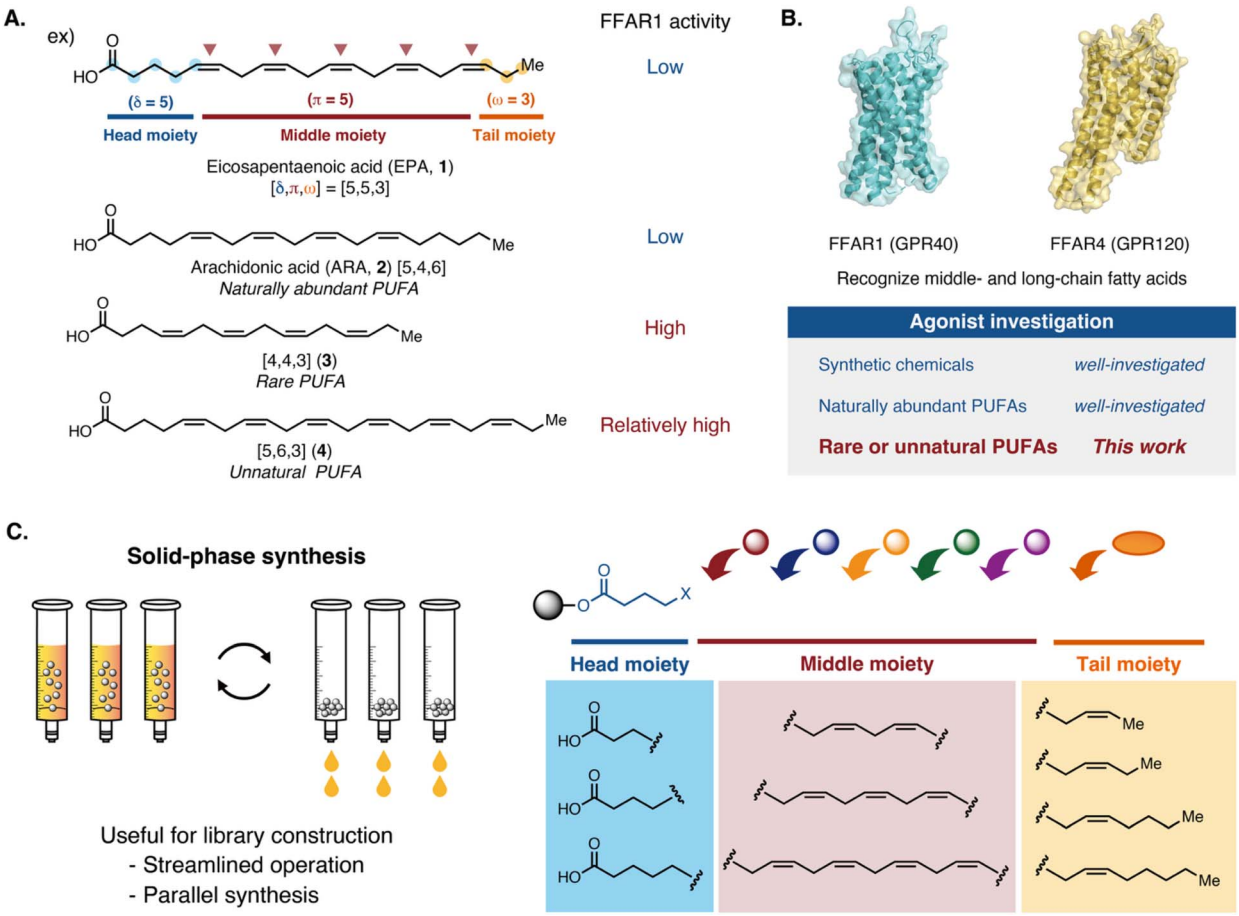

Fig. 1 Schematic illustration of the research background and key technologies in this work. (A) Chemical structures of PUFAs and their FFAR1 agonist activities. (B) Structures of FFAR1 (PDB ID: 4PHU) and FFAR4 (PDB ID: 8ID6), along with research progress of their agonists. (C) Schematic illustration of solid-phase synthesis of PUFAs.[12]

Although some structure–activity relationship (SAR) studies have investigated the relationship between PUFAs and FFAR1/4, existing research has predominantly focused on PUFAs available from nature, leading to an insufficient understanding of SAR (Fig. 1B). Recent findings, however, have demonstrated that FFAR1/4 agonist activity is highly sensitive to subtle structural variations in PUFAs. For instance, Voest and colleagues reported that hexadeca-4,7,10,13-tetraenoic acid ([4,4,3], **3**) exhibits potent FFAR1/4 agonist activity.[11] We also found that FFAR1 agonist activity, specifically $G\alpha_q$ and $G\alpha_{12/13}$ signalling, varies depending on carbon chain length and the number of olefins.[12] Notably, [5,6,3] (**4**), which contains additional olefin and methylene group compared to EPA (**1**), exhibits higher FFAR1 agonist activity than **1**, but lower than **3** (Fig. 1A). These findings underscore the necessity of a comprehensive examination of FFAR1/4 activation by PUFAs, extending beyond commonly available PUFAs to include structurally refined variants that may provide deeper insights into their SAR.

Recently, we developed a solid-phase synthesis approach for PUFAs.[12] Solid-phase synthesis is widely used in the preparation of biopolymers such as peptides and nucleic acids, enabling efficient construction of highly diverse compound libraries.[13–16] However, solid-phase synthesis has rarely been applied to lipids, including PUFAs. The developed method enables the efficient synthesis of PUFAs through streamlined operations and facilitates PUFA library construction containing diverse structures by controlling [δ,π,ω] (Fig. 1C). In contrast to conventional liquid-phase synthesis, which entails highly time-consuming and laborious processes, the solid-phase synthesis approach effectively overcomes these limitations.

In this study, we investigated FFAR1-dependent $G\alpha_q$ and $G\alpha_{12/13}$ signalling, as well as FFAR4-dependent $G\alpha_q$, $G\alpha_{12/13}$, and $G\alpha_o$ signalling, utilizing a compound library comprising 30 PUFAs. Of these, 9 PUFAs were obtained from a commercial supplier, 3 PUFAs were previously reported,[12] and 18 PUFAs were synthesized by the solid-phase synthesis. We selected several PUFAs exhibiting distinct activation profiles on FFAR1/4 and examined their effects on neutrophil pseudopod formation, a process known to be inhibited through FFAR1 activation.[17]

Results and discussion

Construction of PUFA library

We constructed a PUFA library using our solid-phase synthesis approach[12] (Fig. 2), which consists of four sequential steps, with Steps 1–3 defining the parameters δ, π, and ω, respectively.

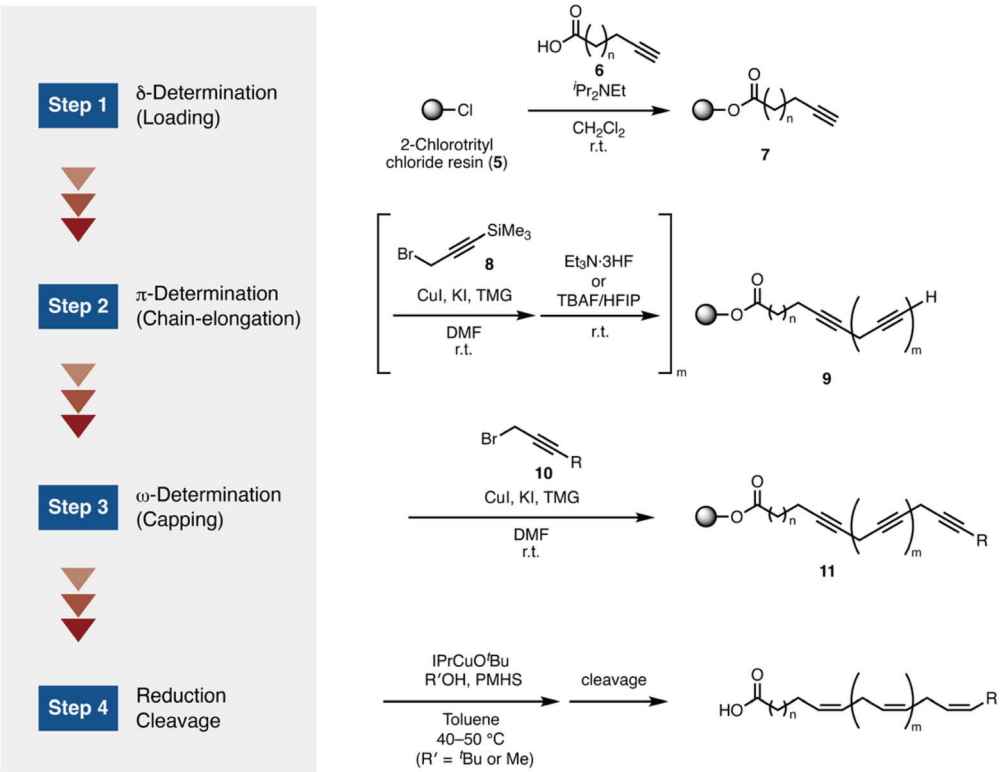

Fig. 2 Solid-phase synthesis of PUFAs.

In Step 1, linear carboxylic acids (C5–12) bearing a terminal alkyne (**6**) were loaded onto polystyrene-based 2-chlorotrityl chloride resin (**5**) (Fig. 2, Step 1). The δ value is determined by the carbon number of the loaded carboxylic acid. Subsequently, the carbon chain was elongated by constructing a skipped diyne framework *via* the nucleophilic addition of copper acetylide to 3-(trimethylsilyl)propargyl bromide (**8**), followed by removing the trimethylsilyl group using $Et_3N{\cdot}3HF$ or tetra-*n*-butylammonium fluoride (TBAF) to regenerate the terminal alkyne (Fig. 2, Step 2). Repeating Step 2, until the desired chain length is achieved, determines the π value. In this study, PUFAs with π = 2–5 were synthesized by repeating Step 2 up to 3 times. Since one alkyne is introduced in both Step 1 and Step 3, the π value is defined as the repetition number of Step 2 (m) plus 2.

Following Step 2, the ω value was defined through a capping reaction on **9** using either propargyl bromide **10** or tosylate with an aliphatic chain, in place of reagent **8** (Fig. 2, Step 3). Finally, the target PUFAs were obtained *via* hydrogen transfer reduction using IPrCuO^{t}Bu, ^{t}BuOH, and polymethylhydrosiloxane (PMHS), followed by cleavage from the solid support (Fig. 2, Step 4). While the previous study exclusively utilized ^{t}BuOH as a proton donor,[12] this study also employed MeOH in some cases.

The PUFAs in this library are summarized in Table 1. This library encompasses PUFAs with $[\delta,\pi,\omega]$ = [4–11,2–6,1–9]. While this library incorporates PUFAs with $[\delta,\pi,\omega]$ = [4–6,3–6,2–6], which was previously investigated for their FFAR1 agonist activity,[12] FFAR4 agonistic activities are newly provided, and the current library expands the explored chemical space (Fig. 3). This expanded library, including PUFAs with $\delta \geq 7$, $\pi \leq 3$, and $\omega = 7$, enables a broader analysis of PUFA structures and their associated biological functions.

Evaluation of FFAR1/4 agonist activity

We evaluated the FFAR1/4 agonist activity of PUFAs in the library using the TGFα shedding assay[18] (Fig. 4). While this assay enables the detection of individual Gα signals from GPCR activation, we specifically measured Gα_q and G$\alpha_{12/13}$ signals for FFAR1 and Gα_q, G$\alpha_{12/13}$, and Gα_o signals for FFAR4. TUG-891, a synthetic agonist for FFAR1 and 4, was used to normalize the measured values.[19]

The results revealed that agonist activity varied depending on subtle differences in carbon chain length (δ), degree of unsaturation (π), and terminal structure (ω) (Fig. 4A).

Among the δ = 4 series, PUFA [4,2,9] (C16), which shares the same δ and π values but has a longer ω than the smallest PUFA in this library, [4,2,2] (C9), exhibited higher agonist activity for FFAR1 ($P < 0.05$ (FFAR1), [4,2,2] *vs.* [4,2,9]). PUFAs [4,3,6] and [4,4,3], which have the same carbon number C16 with [4,2,9], also exhibited higher agonist activities for both FFAR1 and 4 than [4,2,2] ($P < 0.0001$ (FFAR1), $P < 0.0001$ (FFAR4), [4,2,2] *vs.* [4,3,6]; $P < 0.0001$ (FFAR1), $P < 0.0001$ (FFAR4), [4,2,2] *vs.* [4,4,3]). This observation aligns with the known preference of FFAR1 and FFAR4 for long-chain fatty acids.[4,5]

Conversely, among PUFAs with the same total carbon number (C16), [4,3,6], which possesses one additional double

Table 1 Chemical structures of PUFAs in the compound library

[δ,π,ω]	Structure
[4,2,2]	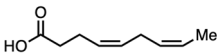
[4,2,9]	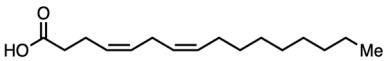
[4,3,6]	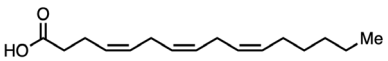
[4,3,9]	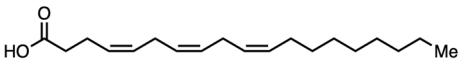
[4,4,3]	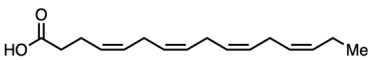
[4,6,3]	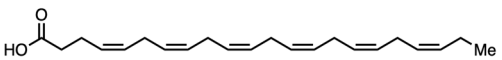
[5,2,9]	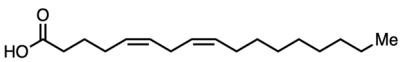
[5,3,3]	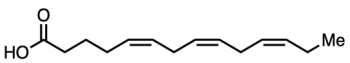
[5,3,6]	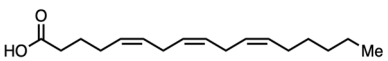
[5,4,2]	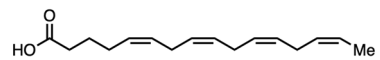
[5,4,6]	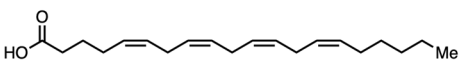
[5,5,2]	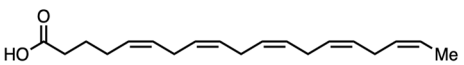
[5,5,3]	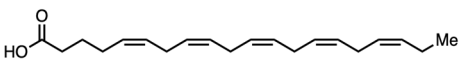
[6,2,2]	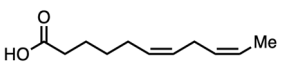
[6,2,9]	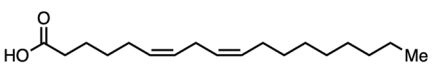
[6,3,3]	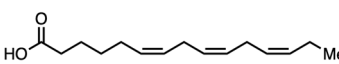
[6,3,6]	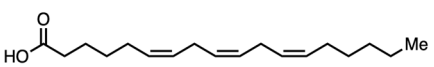
[6,4,3]	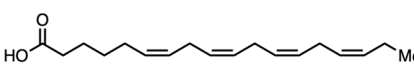
[7,4,6]	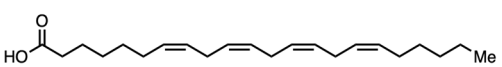
[8,3,6]	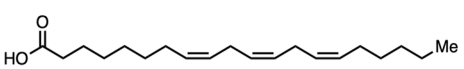

Table 1 (*Contd.*)

[δ,π,ω]	Structure
[9,2,6]	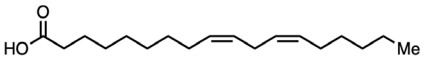
[9,3,3]	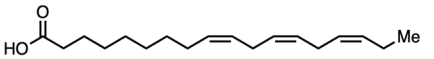
[10,2,1]	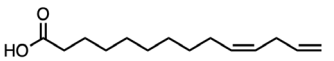
[10,2,2]	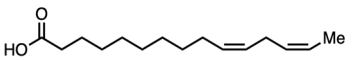
[10,2,3]	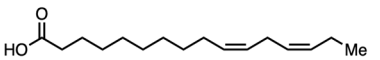
[10,2,6]	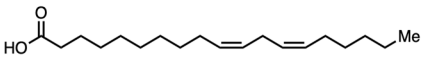
[10,3,2]	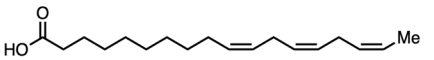
[10,3,3]	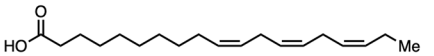
[10,4,2]	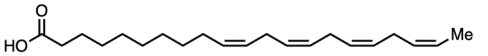
[11,3,3]	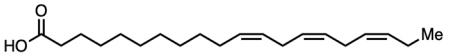

bond and a shorter ω value (by three carbons), exhibited higher FFAR1 agonist activity than [4,2,9], suggesting a preference for increased unsaturation ($P < 0.0001$ (FFAR1), [4,2,9] *vs.* [4,3,6]). However, [4,3,9] (C19), which has an extended carbon chain,

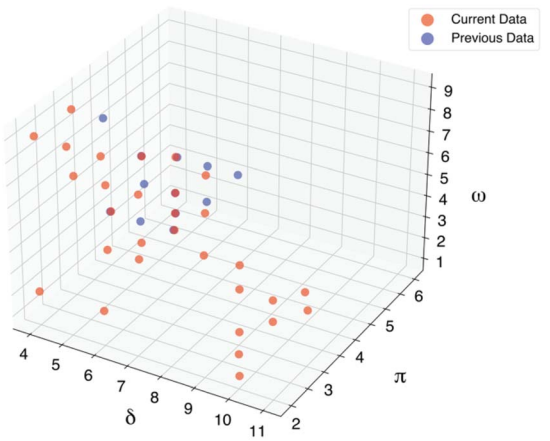

Fig. 3 3D-plot of [δ,π,ω] of each PUFA in the PUFA libraries. The orange circles represent PUFAs only in the current work. The blue circles represent PUFAs only in our previous work.[12] The red circles represent PUFAs in both libraries.

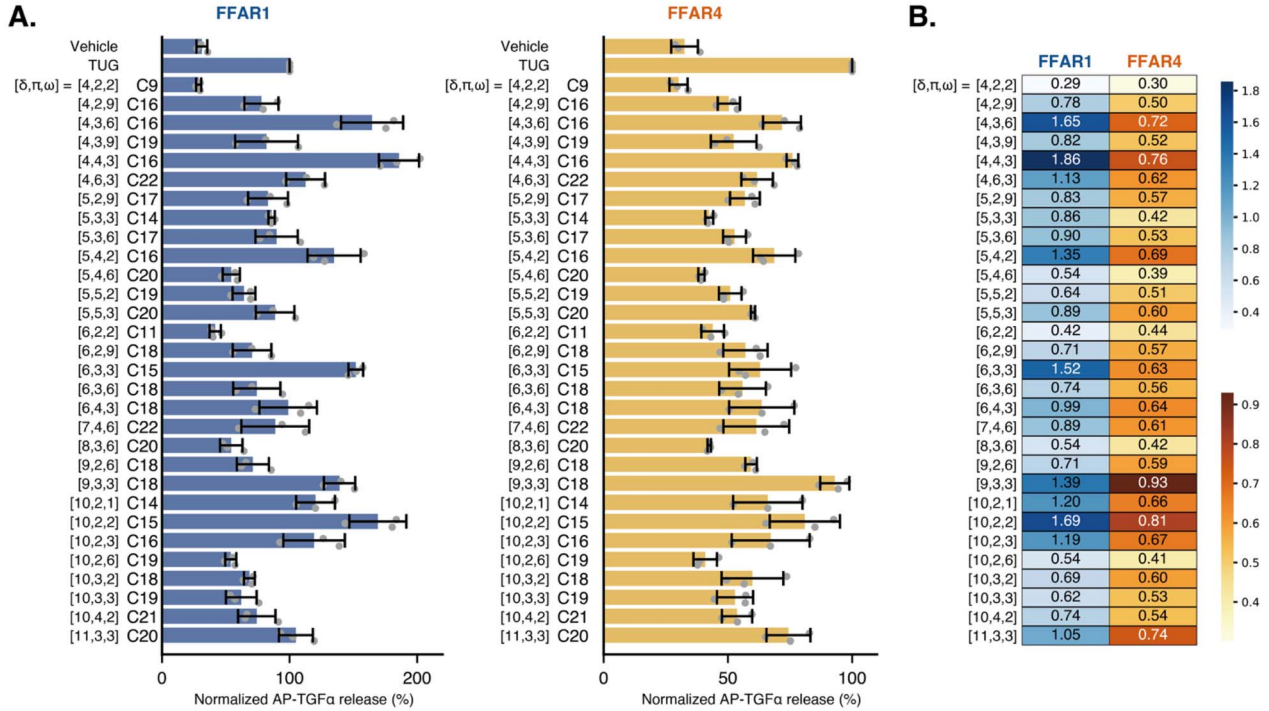

Fig. 4 Activation of FFAR1 and FFAR4 by PUFAs, measured using the TGFα shedding assay. (A) Bar graphs of the activation of FFAR1/4. TUG: TUG-891, a synthetic agonist for FFAR1 and 4.[19] Concentration of TUG: 1.0 μM. Concentration of PUFAs: 3.0 μM. Each point represents an average value obtained from individual experiments (six replicates). Bar graphs show mean values, with error bars representing the standard deviation (SD), $n = 3$. (B) Heat-maps of FFAR1/4 agonist activity shown in (A). The numbers in each box represent mean values of normalized AP-TGFα release, indicating FFAR1/4 agonist activities.

demonstrated reduced activity ($P < 0.0001$ (FFAR1), [4,3,6] *vs.* [4,3,9]), whereas [4,4,3] (C16), which maintains the same chain length as [4,3,6] but with an additional double bond ($\pi = 4$), displayed comparable activity levels.

Among the $\delta = 5$ series, PUFA [5,4,2] (C16) exhibited higher FFAR1 agonist activity than [5,2,9] (C17), [5,3,3] (C14), [5,4,6] (C20), and [5,5,2] (C19) ($P < 0.05$, [5,4,2] *vs.* [5,2,9]; $P < 0.05$, [5,4,2] *vs.* [5,3,3]; $P < 0.0001$, [5,4,2] *vs.* [5,4,6]; $P < 0.0005$, [5,4,2] *vs.* [5,5,2]). This observation is consistent with the trend observed in the $\delta = 4$ series, where C16 PUFAs demonstrated the highest activity. However, the results also suggest that carbon chain length alone does not solely determine activation potency. As mentioned above, [4,3,6] (C16) and [4,4,3] (C16) have higher FFAR1 agonist activities than [4,2,9] (C16). Additionally, in the comparison of PUFAs [4,2,9] (C16) and [5,4,2] (C16), the latter, which possesses a longer δ, higher degree of unsaturation, and a shorter ω, exhibited greater FFAR1 activation ($P < 0.01$ (FFAR1), [4,2,9] *vs.* [5,4,2]). Similarly, while [5,3,3] (C14), which shares the same π value as [5,3,6], displayed comparable activity with [5,3,6], [5,4,2] (C16) demonstrated a more pronounced FFAR1 agonist effect ($P < 0.05$ (FFAR1), [5,3,3] *vs.* [5,4,2]).

Among the $\delta = 6$ series, [6,3,3] exhibited the highest FFAR1 agonist activity. Interestingly, no significant difference was observed in FFAR4 agonist activity in our assay. The C18 PUFA series, [6,2,9], [6,3,6], and [6,4,3] displayed comparable activity. This exemplified a case in which differences in the degree of unsaturation (π) and a terminal segment (ω) do not impact agonist activities. By contrast, a distinct difference was observed in PUFAs with $\delta = 9$, as shown by the comparison between [9,2,6] and [9,3,3] ($P < 0.0005$ (FFAR1), $P < 0.005$ (FFAR4), [9,2,6] *vs.* [9,3,3]). In PUFAs with $\delta = 10$, increasing ω enhanced FFAR1 agonist activity in comparison of [10,2,1] and [10,2,2] ($P < 0.05$ (FFAR1), [10,2,1] *vs.* [10,2,2]), whereas [10,2,3], with longer terminal chain ($\omega = 3$), exhibited decreased activity ($P < 0.05$ (FFAR1), [10,2,2] *vs.* [10,2,3]). Further elongation of the tail moiety to $\omega = 6$, [10,2,6], caused a larger decrease of both FFAR1/4 agonist activities ($P < 0.0001$ (FFAR1), $P < 0.0001$ (FFAR4), [10,2,2] *vs.* [10,2,6]).

In this study, no universal structural features were identified that directly correlate FFAR1/4 agonist activity with the chemical structures of PUFAs. However, among PUFAs with $\delta \leq 9$, there was a tendency for compounds with higher unsaturation (larger π, smaller ω) and chain lengths around C16 to exhibit relatively higher agonist activity. In contrast, for $\delta \geq 10$, compounds with shorter chain lengths (around C15), lower unsaturation (smaller π), and more compact terminal structures (smaller ω) often showed higher activity. Notably, exceptions to these trends were also observed.

Under these experimental conditions, a correlative trend was observed between FFAR1 and FFAR4 agonist activities, where PUFAs with potent FFAR1 activation also exhibited enhanced FFAR4 activation (Fig. 4B). Previous studies investigating naturally abundant PUFAs suggested that FFAR4 preferentially

recognizes longer-chain PUFAs compared to FFAR1.[3–5] When comparing [6,3,3] (C15) and [9,3,3] (C18), which differ in chain length (δ) but share identical π and ω values, [9,3,3] (C18) showed significantly higher activation of FFAR4 than [6,3,3] (C15), whereas FFAR1 was similarly activated by both PUFAs ($P > 0.99$ (FFAR1), $P < 0.01$ (FFAR4), [6,3,3] *vs.* [9,3,3]). However, when [5,3,3] (C14), [6,3,3] (C15), [9,3,3] (C18), [10,3,3] (C19), and [11,3,3] (C20) were compared, both FFAR1 and FFAR4 were activated to a comparable extent. Overall, in this study, utilizing a detection system that measures $G\alpha_q$, $G\alpha_{12/13}$, and $G\alpha_o$ signal in cells transiently overexpressing receptors, no clear difference in chain-length preferences between FFAR1 and FFAR4 was observed. To uncover a more detailed relationship between the structural features and FFAR1/4 preference, further investigations using other evaluation systems and an expanded library are necessary. Nevertheless, this analysis revealed that distinct activation profiles exist among individual PUFAs and that specific chemical structures can confer strong agonist activity for both FFAR1 and FFAR4.

Evaluation of inhibitory effects on neutrophil pseudopod formation and hypersensitivity

Because FFAR1 and 4 are involved in immune regulation, they are attractive therapeutic targets for inflammatory diseases and immune disorders.[4,5,7,20,21] 17,18-EpETE (**12**), derived from EPA (**1**) through epoxidation at C17,18 positions by cytochrome P450 (CYP450), is known to strongly activate FFAR1 in neutrophils (Fig. 5A). This activation inhibits pseudopod formation through Rac suppression, ultimately preventing neutrophil migration and reducing accumulation in inflammatory sites. As a result, **12** exerts a potent anti-inflammatory effect.[17] The PUFAs that exhibited FFAR1 agonist activity in this study may also have the potential to exert anti-inflammatory effects. In addition, investigating the relationship between FFAR4 agonist activity and the ability to inhibit pseudopod formation would be valuable because it has remained unclear to date.[17] We focused in particular on [4,4,3], which demonstrated high FFAR1/4 activation in the present analysis. In our previous study, [4,4,3] was also suggested to have FFAR1 agonist activity comparable to

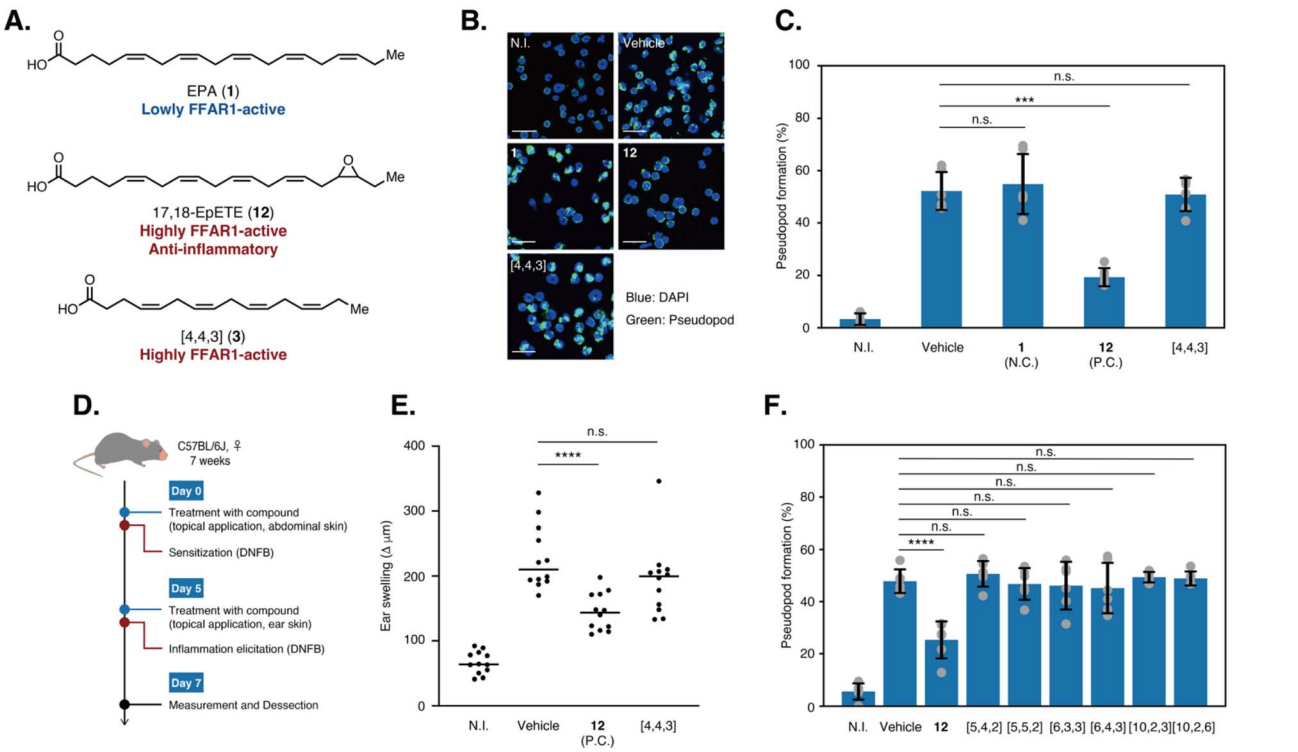

Fig. 5 Investigation of the anti-inflammatory effect of PUFAs. (A) Chemical structures of EPA (**1**), 17,18-EpETE (**12**), and [4,4,3] (**3**). (B) Fluorescent images showing the inhibition of neutrophil pseudopod formation. PUFA concentration: 100 nM. Green: phalloidin indicating the pseudopod formation, Blue: DAPI. Scale bars: 20 μm. N.I.: non LTB_4-induction control. (C) Plots of pseudopod formation of neutrophils. Bar graphs represent averages of values obtained in six independent experiments. Error bars indicate the SD. ***$P < 0.001$, n.s.: not significant. N.I.: non LTB_4-induction control. N.C.: negative control group. P.C.: positive control group. The control data (N.I., Vehicle, **1**, and **12**) are adopted from those described in our previous report.[12] [4,4,3] (**3**) was examined in parallel with these controls under the same experimental settings. (D) Schematic representation of the experimental outline. (E) Plots of ear swelling. Data are combined from three independent experiments, and each point represents data from an individual mouse. Horizontal bars indicate medians. Statistical significance was evaluated by one-way analysis of variance with post-hoc Tukey test for multiple comparisons. N.I.: non DNFB-induction control. P.C.: positive control group. ****$P < 0.0001$, n.s.: not significant. (F) Plots of pseudopod formation of neutrophils. Bar graphs indicate averages of values obtained in six independent experiments. Error bars indicate the SD. ****$P < 0.0001$, n.s.: not significant. N.I.: non LTB_4-induction control.

that of **12**.[12] Therefore, we hypothesized that [4,4,3] would exhibit an anti-inflammatory effect.

To test this hypothesis, we first evaluated the effect of [4,4,3] using neutrophil pseudopod formation assay (Fig. 5B and C). In this assay, pseudopod formation was induced by leukotriene B_4 (LTB_4) stimulation in neutrophils isolated from mouse bone marrow, following pre-treatment with PUFAs or EtOH (vehicle control). After cell fixation, pseudopod formation was assessed *via* F-actin staining. Contrary to our expectations, [4,4,3] did not exhibit pseudopod inhibition even at 100 nM, a concentration at which **12** exerts a significant inhibitory effect.

We next examined whether [4,4,3] could exert anti-inflammatory effects *in vivo*. To evaluate its potential anti-inflammatory properties, we employed a hypersensitivity model in mice (Fig. 5D and E). In this experiment, mice received topical application of PUFAs or EtOH (vehicle control) on the abdominal skin, followed by sensitization with 1-fluoro-2,4-dinitrobenzene (DNFB) on Day 0. On Day 5, hypersensitivity was induced by applying DNFB to the ear 30 minutes after topical administration of PUFAs or EtOH, and ear swelling was measured on Day 7.

When 17,18-EpETE (**12**) was administered at 100 ng per treatment, ear swelling was significantly reduced compared to the vehicle group, consistent with previous reports.[12,17] However, no significant difference was observed between the [4,4,3] and the vehicle group, indicating that despite the FFAR1 agonist activity, [4,4,3] exhibits no anti-inflammatory properties.

Previous studies have suggested that FFAR1 agonist activity plays a crucial role in mediating its anti-inflammatory effects.[17] To further explore this, we examined the inhibitory effects of [5,4,2], [5,5,2], [6,3,3], [6,4,3], [10,2,3], and [10,2,6] on neutrophil pseudopod formation, as they have structural variations and exhibit different patterns of FFAR1/4 agonist activity (Fig. 5F).

At a concentration of 100 nM, none of the tested PUFAs produced a significant reduction in neutrophil pseudopod formation. Interestingly, contrary to our expectations, the PUFA with FFAR1/4 activation ability used in this study did not exhibit inhibitory effects. These findings may suggest that factors other than $G\alpha_q$, $G\alpha_{12/13}$, and $G\alpha_o$ signalling through FFAR1/4 contribute to neutrophil pseudopod formation and the anti-inflammatory response in this hypersensitivity model.

Conclusions

We constructed a PUFA library using solid-phase synthesis and systematically evaluated the FFAR1/4 agonist activities ($G\alpha_q$, $G\alpha_{12/13}$, and $G\alpha_o$ signalling) of 30 PUFAs with varying carbon chain lengths, degrees of unsaturation, and positional distributions of double bonds. We selected six PUFAs from the library and examined their anti-inflammatory effects in mouse neutrophils and mouse model of hypersensitivity.

Despite exhibiting varying degrees of FFAR1/4 agonist activity, none of the tested PUFAs showed anti-inflammatory effects. Although it has been suggested that the anti-inflammatory effect is mediated by activation of FFAR1,[17] our results suggest that the suppression of neutrophil pseudopod formation and its associated anti-inflammatory response is not solely governed by FFAR1 activation. Instead, alternative signalling pathways independent of FFAR1 agonism and/or FFAR1-mediated signals beyond $G\alpha_q$ and $G\alpha_{12/13}$, measured in our TGFα shedding assay, may play a critical role.

Future research will require a comprehensive analysis of the structural determinants of PUFA-mediated anti-inflammatory effects through an expanded PUFA library, where chemical structures are precisely defined. In addition to the structural features described here, the effects of other structural factors, such as *cis*/*trans*-configurations, should also be investigated. In particular, it would be of interest to investigate whether the observed biological activities of individual PUFAs arise from their intrinsic agonist activity toward FFARs or are influenced by physicochemical properties such as solubility and aggregation behavior. Computational approaches, including docking-based binding energy estimation, could offer further insights.

This study highlights the utility of PUFA solid-phase synthesis as a powerful approach for elucidating the relationship between PUFA chemical structures and their biological functions.

Experimental

Animal experiments

All experiments involving mice were conducted in accordance with the guidelines of the Animal Care and Use Committee of National Institutes of Biomedical Innovation, Health and Nutrition (NIBN) and the Committee on the Ethics of Animal Experiments of National Institutes of Biomedical Innovation, Health and Nutrition (NIBN) (approval no. DSR04-37R7).

Neutrophil pseudopod formation inhibition (Fig. 5B and C). The experiments were conducted according to our previous report.[12] Neutrophil pseudopod was stained with phalloidin. Neutrophils were treated with PUFAs for 15 min before stimulation with LTB_4. The final concentration of PUFA was 100 nM. EtOH was used for the Vehicle group.

Evaluation of anti-inflammatory effect *in vivo* (Fig. 5D–F). The experiments were conducted according to our previous report.[12] Mice were treated with either **12** (100 ng in DPBS), **3** (100 ng in DPBS), or vehicle (50% EtOH in DPBS) by topical application on the abdominal skin; on Day 5, mice were then stimulated with DNFB 30 min after topical application with the corresponding PUFA or vehicle (the same dose as Day 0) on the ear skin. Ear swelling was evaluated on Day 7.

Author contributions

Y. Sa. and S. S. conceived and designed the project.; Y. Sh. synthesized PUFAs and collected compound data with the help of Y. Sa. and S. S.; Y. Sh. performed TGFα shedding assay with the help of Y. Sa., M. A., A. U., J. A., and S. S.; M. H. performed cell experiments and animal experiments with the help of J. K.; Y. Sh., Y. Sa., and S. S. wrote the manuscript, which was edited by all co-authors.

Conflicts of interest

The authors declare the following competing financial interest: the authors (Y. Sh., Y. Sa., M. A., and S. S.) have filed a patent application related to the preparation method of polyunsaturated fatty acids on solid-phase (Patent applicant: The University of Tokyo; Inventors: Yutaro Saito, Shinsuke Sando, Mayuko Akita, Yusuke Sano, Yaohong Shi; Application number: PCT/JP2025/011856; Current application status: pending). All other authors declare they have no competing interests.

Data availability

The data supporting this article have been included as part of the SI. Source data for the assays in this article are available at the UTokyo Repository at **https://doi.org/10.15083/0002013669**. See DOI: **https://doi.org/10.1039/d5ra04836b**.

Acknowledgements

This work was performed in part at One-stop Sharing Facility Center for Future Drug Discoveries in Graduate School of Pharmaceutical Sciences, the University of Tokyo. This work was supported by JSPS KAKENHI [grant numbers JP23KJ0751 (Y. Sh.), JP22K14780 (to Y. Sa.) and JP25K01889 (to Y. Sa.)]; AMED [grant numbers JP233fa727001 (to Y. Sa. and J. K.)]; Toyota Riken Scholar Program (to Y. Sa.); Mizuho Foundation for the Promotion of Sciences (to Y. Sa.); KONICA MINOLTA Award in Synthetic Organic Chemistry, Japan (to Y. Sa.); and JST-CREST [grant number JPMJCR21N5 (to S. S.)].

Notes and references

1 S. C. Dyall, L. Balas, N. G. Bazan, J. T. Brenna, N. Chiang, F. da Costa Souza, J. Dalli, T. Durand, J. M. Galano, P. J. Lein, C. N. Serhan and A. Y. Taha, *Prog. Lipid Res.*, 2022, **86**, 101165.
2 R. K. Saini and Y. S. Keum, *Life Sci.*, 2018, **203**, 255–267.
3 E. Christiansen, K. R. Watterson, C. J. Stocker, E. Sokol, L. Jenkins, K. Simon, M. Grundmann, R. K. Petersen, E. T. Wargent, B. D. Hudson, E. Kostenis, C. S. Ejsing, M. A. Cawthorne, G. Milligan and T. Ulven, *Br. J. Nutr.*, 2015, **113**, 1677–1688.
4 G. Milligan, B. Shimpukade, T. Ulven and B. D. Hudson, *Chem. Rev.*, 2017, **117**, 67–110.
5 I. Kimura, A. Ichimura, R. Ohue-Kitano and M. Igarashi, *Physiol. Rev.*, 2020, **100**, 171–210.
6 A. Ichimura, A. Hirasawa, O. Poulain-Godefroy, A. Bonnefond, T. Hara, L. Yengo, I. Kimura, A. Leloire, N. Liu, K. Iida, H. Choquet, P. Besnard, C. Lecoeur, S. Vivequin, K. Ayukawa, M. Takeuchi, K. Ozawa, M. Tauber, C. Maffeis, A. Morandi, R. Buzzetti, P. Elliott, A. Pouta, M. R. Jarvelin, A. Körner, W. Kiess, M. Pigeyre, R. Caiazzo, W. Van Hul, L. Van Gaal, F. Horber, B. Balkau, C. Lévy-Marchal, K. Rouskas, A. Kouvatsi, J. Hebebrand, A. Hinney, A. Scherag, F. Pattou, D. Meyre, T. A. Koshimizu, I. Wolowczuk, G. Tsujimoto and P. Froguel, *Nature*, 2012, **483**, 350–354.
7 A. Bartoszek, E. Von Moo, A. Binienda, A. Fabisiak, J. B. Krajewska, P. Mosińska, K. Niewinna, A. Tarasiuk, K. Martemyanov, M. Salaga and J. Fichna, *Pharmacol. Res.*, 2020, **152**, 104604.
8 Y. Itoh, Y. Kawamata, M. Harada, M. Kobayashi, R. Fujii, S. Fukusumi, K. Ogi, M. Hosoya, Y. Tanaka, H. Uejima, H. Tanaka, M. Maruyama, R. Satoh, S. Okubo, H. Kizawa, H. Komatsu, F. Matsumura, Y. Noguchi, T. Shinohara, S. Hinuma, Y. Fujisawa and M. Fujino, *Nature*, 2003, **422**, 173–176.
9 K. Kotarsky, N. E. Nilsson, E. Flodgren, C. Owman and B. Olde, *Biochem. Biophys. Res. Commun.*, 2003, **301**, 406–410.
10 C. P. Briscoe, M. Tadayyon, J. L. Andrews, W. G. Benson, J. K. Chambers, M. M. Eilert, C. Ellis, N. A. Elshourbagy, A. S. Goetz, D. T. Minnick, P. R. Murdock, H. R. Sauls, U. Shabon, L. D. Spinage, J. C. Strum, P. G. Szekeres, K. B. Tan, J. M. Way, D. M. Ignar, S. Wilson and A. I. Muir, *J. Biol. Chem.*, 2003, **278**, 11303–11311.
11 J. M. Houthuijzen, I. Oosterom, B. D. Hudson, A. Hirasawa, L. G. M. Daenen, C. M. McLean, S. V. F. Hansen, M. T. M. Van Jaarsveld, D. S. Peeper, S. J. Sadatmand, J. M. L. Roodhart, C. H. A. Van De Lest, T. Ulven, K. Ishihara, G. Milligan and E. E. Voest, *FASEB J.*, 2017, **31**, 2195–2209.
12 Y. Saito, M. Akita, A. Saika, Y. Sano, M. Hotta, J. Morimoto, A. Uwamizu, J. Aoki, T. Nagatake, J. Kunisawa and S. Sando, *Nat. Chem.*, 2025, DOI: **10.1038/s41557-025-01853-5**.
13 R. B. Merrifield, *J. Am. Chem. Soc.*, 1963, **85**, 2149–2154.
14 S. L. Pedersen, A. P. Tofteng, L. Malik and K. J. Jensen, *Chem. Soc. Rev.*, 2012, **41**, 1826–1844.
15 A. Adak, G. Das, V. Gupta, J. Khan, N. Mukherjee, P. Mondal, R. Roy, S. Barman, P. K. Gharai and S. Ghosh, *J. Med. Chem.*, 2022, **65**, 13866–13878.
16 S. L. Beaucage and M. H. Caruthers, *Tetrahedron Lett.*, 1981, **22**, 1859–1862.
17 T. Nagatake, Y. Shiogama, A. Inoue, J. Kikuta, T. Honda, P. Tiwari, T. Kishi, A. Yanagisawa, Y. Isobe, N. Matsumoto, M. Shimojou, S. Morimoto, H. Suzuki, S. ichiro Hirata, P. Steneberg, H. Edlund, J. Aoki, M. Arita, H. Kiyono, Y. Yasutomi, M. Ishii, K. Kabashima and J. Kunisawa, *J. Allergy Clin. Immunol.*, 2018, **142**, 470–484.
18 A. Inoue, J. Ishiguro, H. Kitamura, N. Arima, M. Okutani, A. Shuto, S. Higashiyama, T. Ohwada, H. Arai, K. Makide and J. Aoki, *Nat. Methods*, 2012, **9**, 1021–1029.
19 B. Shimpukade, B. D. Hudson, C. K. Hovgaard, G. Milligan and T. Ulven, *J. Med. Chem.*, 2012, **55**, 4511–4515.
20 L. Sheng Zhang, Z. Shou Zhang, Y. Zhu Wu, B. Guo, J. Li, X. Qi Huang, F. Min Zhang, M. Yao Li, P. Chang Yang and X. Bao Zheng, *Int. Immunopharmacol.*, 2024, **130**, 111778.
21 M. Lückmann, A. Shenol, T. A. D. Nissen, J. E. Petersen, D. Kouvchinov, T. W. Schwartz and T. M. Frimurer, *ACS Med. Chem. Lett.*, 2022, **13**, 1839–1847.